

RESEARCH ARTICLE

A multicomponent model of phytoplankton size structure

10.1002/2014JC009859

Key Points:

- A published model is tested using two estimates of size-fractionated chlorophyll
- A new model is developed to estimate multiple size fractions
- The new model was found to be consistent with a traditional size-spectra model

Supporting Information:

- Readme
- Supporting figure
- Supporting tables

Correspondence to:

R. J. W. Brewin,
robbr@pml.ac.uk

Citation:

Brewin, R. J. W., S. Sathyendranath, G. Tilstone, P. K. Lange, and T. Platt (2014), A multicomponent model of phytoplankton size structure, *J. Geophys. Res. Oceans*, 119, doi:10.1002/2014JC009859.

Received 31 JAN 2014

Accepted 8 MAY 2014

Accepted article online 12 MAY 2014

Robert J. W. Brewin^{1,2}, Shubha Sathyendranath^{1,2}, Gavin Tilstone¹, Priscila K. Lange³, and Trevor Platt¹
¹Plymouth Marine Laboratory, Prospect Place, The Hoe, Plymouth, UK, ²National Centre for Earth Observation, Plymouth Marine Laboratory, Plymouth, UK, ³Laboratório de Fitoplâncton e Microorganismos Marinhos, Instituto de Oceanografia, Universidade Federal do Rio Grande, Av. Itália, Km 8, Rio Grande/RS, Brazil

Abstract Size-fractionated filtration (SFF) is a direct method for estimating pigment concentration in various size classes. It is also common practice to infer the size structure of phytoplankton communities from diagnostic pigments estimated by high-performance liquid chromatography (HPLC). In this paper, the three-component model of Brewin et al. (2010) was fitted to coincident data from HPLC and from SFF collected along Atlantic Meridional Transect cruises. The model accounted for the variability in each data set, but the fitted model parameters differed for the two data sets. Both HPLC and SFF data supported the conceptual framework of the three-component model, which assumes that the chlorophyll concentration in small cells increases to an asymptotic maximum, beyond which further increase in chlorophyll is achieved by the addition of larger celled phytoplankton. The three-component model was extended to a multicomponent model of size structure using observed relationships between model parameters and assuming that the asymptotic concentration that can be reached by cells increased linearly with increase in the upper bound on the cell size. The multicomponent model was verified using independent SFF data for a variety of size fractions and found to perform well ($0.628 \leq r \leq 0.989$) lending support for the underlying assumptions. An advantage of the multicomponent model over the three-component model is that, for the same number of parameters, it can be applied to any size range in a continuous fashion. The multicomponent model provides a useful tool for studying the distribution of phytoplankton size structure at large scales.

1. Introduction

The size of phytoplankton plays a fundamental role in marine ecology and biogeochemical cycling [Chisholm, 1992]. Light energy absorbed by phytoplankton may be used for photosynthesis or dissipated as heat. The absorption of light by an assemblage of phytoplankton varies according to its size structure [Morel and Bricaud, 1981; Prieur and Sathyendranath, 1981; Ciotti et al., 1999; Bricaud et al., 2004; Devred et al., 2006]. Therefore, phytoplankton size influences both the photosynthetic rate of the phytoplankton and the rate of heating of the upper layer of the ocean [Sathyendranath and Platt, 2007; Uitz et al., 2008]. Phytoplankton physiology, nutrient uptake, growth rates, and metabolic rates are also in part controlled by the size of phytoplankton [Platt and Denman, 1976, 1977, 1978; Probyn, 1985; Geider et al., 1986; Chisholm, 1992; Sunda and Huntsman, 1997; Raven, 1998]. Large-celled phytoplankton are thought to be mostly responsible for new or nitrate-based production; much of the vertical flux of particles from the surface mixed layer; and deep-ocean carbon export [McCave, 1975; Eppley and Peterson, 1979; Michaels and Silver, 1988; Boyd and Newton, 1999; Laws et al., 2000; Guidi et al., 2009; Uitz et al., 2010; Briggs et al., 2011]. There is evidence that the size structure of phytoplankton influences the structure of the marine food chain [Maloney and Field, 1991; Legendre and LeFevre, 1991] and its trophic pathways [Parsons and Lalli, 2002]. A size-based partitioning of phytoplankton can capture key phytoplankton traits in relation to marine biogeochemical cycling [Nair et al., 2008; Marañón, 2009] and has been adopted in many large-scale marine biogeochemical models [e.g., Aumont et al., 2003; Blackford et al., 2004; Kishi et al., 2007; Marinov et al., 2010; Ward et al., 2012].

Due to the paucity of in situ data on phytoplankton size, coupled with an increasing demand for observations on phytoplankton size that are highly resolved in time and space [e.g., from the biogeochemical modeling community, see Ward et al., 2012; Hirata et al., 2013], increasing efforts have been made to tie the size structure of the phytoplankton to optical or biogeochemical variables that are, or can be, measured at high

resolution in time and space (using in situ or remote-sensing methods). Observations of the chlorophyll concentration [e.g., *Uitz et al.*, 2006; *Hirata et al.*, 2008, 2011; *Brewin et al.*, 2010], the magnitude or shape of the phytoplankton absorption (a_{ph}) spectrum [e.g., *Sathyendranath et al.*, 2004; *Ciotti and Bricaud*, 2006; *Devred et al.*, 2006, 2011; *Aiken et al.*, 2007, 2008; *Hirata et al.*, 2008; *Mouw and Yoder*, 2010; *Fujiwara et al.*, 2011; *Bricaud et al.*, 2012], and the shape of the particulate backscattering (b_{bp}) spectrum [e.g., *Loisel et al.*, 2006; *Kostadinov et al.*, 2009; *Fujiwara et al.*, 2011] have recently been proposed as indices of size structure by, either empirically or analytically, relating the size structure of the phytoplankton to the variable of interest.

Size-fractionated chlorophyll concentrations are of particular interest to the biogeochemical community as they may be used along with suitable photophysiological parameters to estimate size-fractionated primary production using satellite observations [*Claustre et al.*, 2005; *Silió-Calzada et al.*, 2008; *Uitz et al.*, 2008, 2009, 2010], estimate export production [*Guidi et al.*, 2009], used to validate biogeochemical models [*Ward et al.*, 2012; *Hirata et al.*, 2013], or potentially feed into size-based food-web models to forecast the effects of climate change on marine communities [e.g., *Blanchard et al.*, 2012; *Woodworth-Jefcoats et al.*, 2012]. A common method to estimate size-fractionated chlorophyll is to develop statistical links between the total chlorophyll concentration and size structure estimated from HPLC analysis [*Vidussi et al.*, 2001; *Uitz et al.*, 2006; *Brewin et al.*, 2010; *Hirata et al.*, 2011]. Once these statistical links are established, measurements of total chlorophyll concentration (in situ or remotely sensed) are used to infer how chlorophyll is distributed among phytoplankton of various sizes.

Uitz et al. [2006] used a large database of high-performance liquid chromatography (HPLC) measurements (case 1 waters exclusively) to establish statistical links between the surface chlorophyll concentration and the vertical distribution of chlorophyll for different size fractions. HPLC data were partitioned as coming from stratified or mixed waters (based on the ratio of the euphotic depth to the mixed-layer depth) and class intervals in surface chlorophyll concentrations were used to partition stratified and mixed waters into trophic categories. For each category, an associated mean size structure was determined from the in situ HPLC data using specific biomarker pigments [*Vidussi et al.*, 2001]. *Hirata et al.* [2011] related the fractional contribution of three phytoplankton size classes to the total chlorophyll using a suite of empirical functions applied to a global database of HPLC measurements. Using HPLC measurements from the Atlantic Ocean, *Brewin et al.* [2010] fitted a conceptual three-component model tying size fractions of chlorophyll to the total chlorophyll concentration, based on the work of *Sathyendranath et al.* [2001]. Their model describes how phytoplankton size classes are expected to change with chlorophyll concentration and assumes small cells increase in concentration to an upper limit, beyond which chlorophyll may increase only through the addition of larger size classes [*Raimbault et al.*, 1988].

Approaches that make use of HPLC measurements to infer size structure are, as developed by *Vidussi et al.* [2001], limited to three size classes of phytoplankton (pico, $<2 \mu\text{m}$; nano, $2\text{--}20 \mu\text{m}$; and micro, $>20 \mu\text{m}$). Comparisons between HPLC and other estimates of size-fractionated chlorophyll have rarely been conducted (but see *Uitz et al.* [2009] and *Brewin et al.* [2014]), raising a number of questions: Would the conceptual framework of the *Brewin et al.* [2010] model be robust against estimates of size classes that were not based on HPLC data? Could the model be extended to multiple size classes rather than be limited to a small number of discrete size classes?

In this paper, we fit the three-component model of *Brewin et al.* [2010] to both HPLC and SFF measurements, to test the robustness of its conceptual framework for both independent estimates of chlorophyll partitioned into three size classes. The model is then extended to a multicomponent model of size structure that may be used to infer from the total chlorophyll concentration an arbitrary suite of user-specified size fractions. The model is validated using independent measurements of size-fractionated chlorophyll and compared with a biomass size-spectra model. Finally, the parameters of the model are interpreted with respect to the role of bottom-up (nutrients, light) and top-down (grazing) controls on phytoplankton size structure.

2. Data and Methods

We made use of 1445 size-fractionated fluorometric chlorophyll (SFF) measurements taken over a 17 year period (1996–2012) onboard 11 Atlantic Meridional Transect (AMT) cruises (Figure 1 and Table 1).

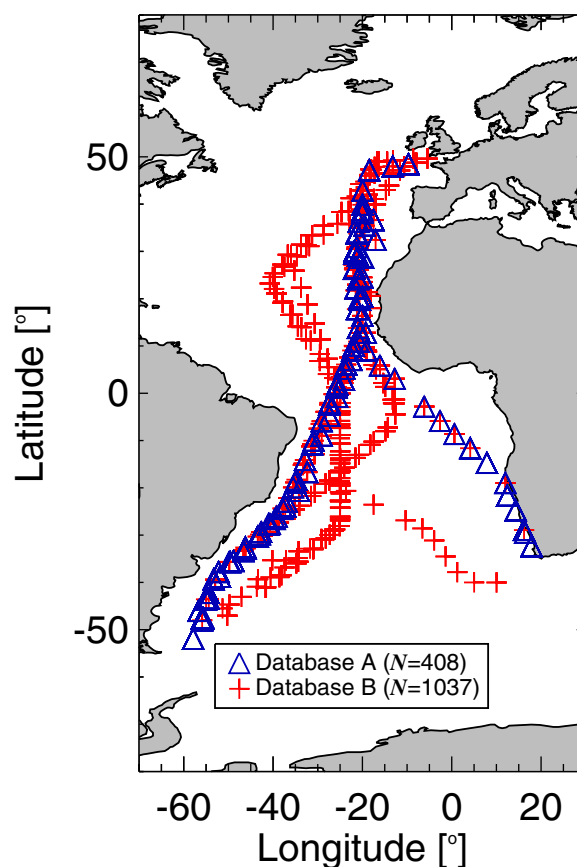


Figure 1. Locations of in situ data used in this study.

2.1. Size-Fractionated Filtration

During these cruises, ~200–300 mL samples were sequentially filtered through different-sized polycarbonate filters. For AMT cruises 2, 3, 4, 5, 6 and 11, 20 μm , 2 μm , and 0.2 μm pore size filters were used, for AMT cruises 13 and 14, 10 μm , 5 μm , 2 μm , and 0.2 μm pore size filters were used, for AMT cruises 15 and 19, 2 μm and 0.2 μm pore size filters were used, and for AMT cruise 22, 10 μm , 2 μm , and 0.2 μm pore size filters were used (Table 1).

After filtration, pigments were extracted by storing the filters in 90% acetone at -20°C between 10 and 24 h [Marañón *et al.*, 2001; Serret *et al.*, 2001]. A Turner Design Fluorometer (either 10 AU, TD-700 or Trilogy) was used to derive the chlorophyll concentration. For each cruise, the fluorometer was precalibrated and postcalibrated with pure chlorophyll *a* as a standard, minimizing differences among cruises and ensuring a consistent methodology over the 17 year time period. The total chlorophyll concentration for SFF was taken as the sum of the size fractions. Figure 1 and Table 1 show the geographical distribution and number of samples for each cruise, respectively.

Picoplankton chlorophyll (C_p) was designated as the concentration of chlorophyll

passing through the 2 μm filter, combined pico-nanoplankton chlorophyll ($C_{p,n}$) was designated as the concentration of chlorophyll passing through the 20 μm filter, microplankton chlorophyll (C_m) was designated as the concentration of chlorophyll retained on the 20 μm filter, and nanoplankton chlorophyll (C_n) was designated as the concentration of chlorophyll retained on the 2 μm filter having passed through the 20 μm filter.

2.2. High-Performance Liquid Chromatography

For AMT cruises with SFF data filtered at 20, 2, and 0.2 μm pore sizes, concurrent HPLC data were extracted where available (Table 1). These HPLC data were processed using methods reported by Barlow *et al.* [1997,

Table 1. AMT Data Used in This Study

AMT	Year	Total Samples	Database A ^a	Database B ^b	SFF Size Fractions
2	1996	105	35	70	<2 μm , 2–20 μm , >20 μm
3	1996	144	91	53	<2 μm , 2–20 μm , >20 μm
4	1997	131	88	43	<2 μm , 2–20 μm , >20 μm
5	1997	129	105	24	<2 μm , 2–20 μm , >20 μm
6	1998	135	89	46	<2 μm , 2–20 μm , >20 μm
11	2000	245		245	<2 μm , 2–20 μm , >20 μm
13	2003	74		74	<2 μm , 2–5 μm , 5–10 μm , >10 μm
14	2004	140		140	<2 μm , 2–5 μm , 5–10 μm , >10 μm
15	2004	41		41	<2 μm , >2 μm
19	2009	225		225	<2 μm , >2 μm
22	2012	76		76	<2 μm , 2–10 μm , >10 μm

^aDatabase A includes measurements with corresponding HPLC data and SFF data at the following three size fractions <2 μm , 2–20 μm , and >20 μm , in addition to measurements of optical depth (τ).

^bDatabase B includes SFF measurements from AMT cruises 2–6 without corresponding HPLC data, and additional SFF data collected on AMT 11, 13, 14, 15, 19, and 22. These samples were used for model validation.

2002, 2004] and *Gibb et al.* [2000], consistent with SCOR/UNESCO recommendations [Jeffrey and Mantoura, 1997; Aiken et al., 2009]. Only those HPLC data for which the total chlorophyll concentration was greater than 0.01 mg m^{-3} , and the difference between the total chlorophyll concentration and the total accessory pigments was less than 30% of the total pigment concentration [Aiken et al., 2009], were used. These methods were designed to control quality of the pigment data, through removing data at unrealistically low chlorophyll concentrations and data in which chlorophyll and the sum of the concentrations of the major accessory pigments did not covary in a predictable manner [Trees et al., 2000].

To estimate the chlorophyll concentration of picoplankton (C_p), nanoplankton (C_n), and microplankton (C_m) from the HPLC data, the approach of *Brewin et al.* [2010] was used. This involved (i) selecting seven diagnostic pigments (fucoxanthin, peridinin, 19'-hexanoyloxyfucoxanthin, 19'-butanoyloxyfucoxanthin, alloxanthin, chlorophyll *b* and divinyl chlorophyll *b*, and zeaxanthin) following the method of *Vidussi et al.* [2001]; (ii) estimating the fraction of picoplankton (F_p), nanoplankton (F_n), and microplankton (F_m) in the total chlorophyll concentration, using the seven diagnostic pigments and the approach of *Uitz et al.* [2006], as modified by *Brewin et al.* [2010]; and (iii) multiplying the fractions of each size class by the total HPLC chlorophyll concentration (C) to estimate C_p , C_n , and C_m . A more detailed description of this procedure is provided in *Brewin et al.* [2010]. For each HPLC measurement sampled at a given depth (z), the optical depth ($\tau = 4.6z/Z_p$) was estimated by computing the euphotic depth (Z_p) from the surface HPLC chlorophyll concentration ($<10 \text{ m}$) using the model of *Morel et al.* [2007]. A total of 408 HPLC samples, with concurrent SFF and τ data, were available for further analysis [see *Brewin et al.*, 2014, for further detail on this data set].

2.3. Partitioning of Data for Model Parameterization and Validation

For model parameterization, the 408 samples with concurrent HPLC, SFF, and τ data were used. This data set is hereinafter referred to as Database A and was designed to investigate whether the conceptual framework of the three-component model of *Brewin et al.* [2010] is supported by both SFF and HPLC data, and to investigate variations in model parameters between two optical layers ($\tau \geq 2.8$ and $\tau < 2.8$, each with a similar number of samples).

For model validation, an independent database of SFF measurements was set aside, hereinafter referred to as Database B. This database contained the original 1445 SFF measurements, from which the 408 measurements in Database A were removed, leaving 1037 measurements. Database B contained SFF chlorophyll measurements at $<2 \mu\text{m}$, $<5 \mu\text{m}$, $<10 \mu\text{m}$, $<20 \mu\text{m}$, $>2 \mu\text{m}$, $>5 \mu\text{m}$, $>10 \mu\text{m}$, $>20 \mu\text{m}$, $2-5 \mu\text{m}$, $2-10 \mu\text{m}$, $5-10 \mu\text{m}$, and $2-20 \mu\text{m}$ and was used strictly to validate the multicomponent model of phytoplankton size structure described in section 3. The geographical distribution and number of samples of these two databases are provided in Figure 1 and Table 1.

2.4. Statistical Tests

To assess the performance of the multicomponent model described in section 3, the Pearson linear correlation coefficient (r), the centre-patterned (or unbiased) root-mean-square error (Ψ), and the bias (δ) were used. The Ψ and δ were computed as

$$\Psi = \left(\frac{1}{N} \sum_{i=1}^N \left\{ \left[X_{i,E} - \left(\frac{1}{N} \sum_{j=1}^N X_{j,E} \right) \right] - \left[X_{i,M} - \left(\frac{1}{N} \sum_{k=1}^N X_{k,M} \right) \right] \right\}^2 \right)^{1/2}, \quad (1)$$

$$\delta = \frac{1}{N} \sum_{i=1}^N (X_{i,E} - X_{i,M}), \quad (2)$$

where X is the chlorophyll concentration and N the number of samples. The subscript M denotes the measured variable and E the estimated variable from the model. Considering that the chlorophyll concentration is approximately log-normally distributed over the global ocean [Campbell, 1995], all statistical tests were performed in \log_{10} space.

3. Model Development

Based on the work of *Sathyendranath et al.* [2001], *Brewin et al.* [2010] proposed a three-component model to estimate the chlorophyll concentrations of three phytoplankton size classes (pico, $<2 \mu\text{m}$; nano, $2-20 \mu\text{m}$;

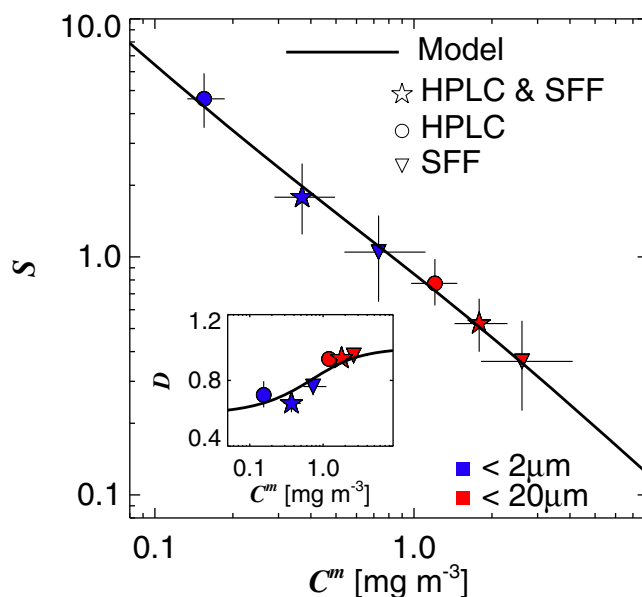


Figure 2. Relationships between the parameters of equation (3). The parameter C^m is the asymptotic maximum chlorophyll concentration for the phytoplankton population i (with $i =$ either $<2 \mu\text{m}$ (blue) or $<20 \mu\text{m}$ (red)), and S determines the initial increase in C for the phytoplankton population i as a function of total chlorophyll (C). The inset shows the relationship between the parameter D ($C^m S$) and C^m for the phytoplankton population i .

and micro, $>20 \mu\text{m}$) as a function of total chlorophyll. The model is based on an exponential function [Sathyendranath *et al.*, 2001] where the chlorophyll concentration of a phytoplankton population lower than a specific size is expressed as

$$C_i = C_i^m [1 - \exp(-S_i C)], \quad (3)$$

where the subscript i refers to a population of phytoplankton with cell size smaller than i (with $i = 2$ or 20 , with the numbers representing size in micrometers), C_i^m is the asymptotic maximum chlorophyll concentration for the phytoplankton population i , and S_i determines the initial increase in C_i with C . If the two values of C_i are known, the chlorophyll concentration in the third size class can be estimated by difference, from the total chlorophyll concentration.

The model of Brewin *et al.* [2010] has been fitted to, and validated with, a

number of different HPLC data sets over the global ocean [Brewin *et al.*, 2010, 2011, 2012a, 2012b; Brotas *et al.*, 2013] but not with size-fractionated filtration (SFF) data. Here for the first time, we fit the model to SFF data. To derive model parameters (C_i^m and S_i , for $i = [2, 20]$), equation (3) was fitted to C , $C_{p,n}$, and C_p derived from the SFF data in Database A. The fitting procedure used a standard, nonlinear least squares method (Levenberg-Marquardt, IDL Routine MPFITFUN [Moré, 1978; Markwardt, 2008]). To avoid the undue influence of large chlorophyll values on the parameterization of the model, the fitting procedure was applied to \log_{10} -transformed data. In addition to fitting the model to SFF data, we also fitted it to C , $C_{p,n}$, and C_p derived from HPLC data and a combination of both HPLC and SFF data in Database A. This was conducted for all measurements, and for data partitioned according to optical depths <2.8 and ≥ 2.8 .

As the chlorophyll concentration tends toward zero, the derivative of equation (3) can be expressed according to

$$\left. \frac{dC_i}{dC} \right|_{C \rightarrow 0} = S_i C_i^m. \quad (4)$$

The product $S_i C_i^m$ is hereafter denoted D_i . Note that D_i should never exceed one, as it would imply small size-fractionated chlorophyll (C_i) is increasing faster than total chlorophyll (C). When fitting equation (3), D_i was constrained to be ≤ 1 . We also used the method of bootstrapping [Efron, 1979] to compute model parameters and their uncertainties. This involved randomly subsampling the data (1000 times) and refitting equation (3) for each subsample. From the resulting parameter distribution, median values and 95% confidence intervals were computed.

Parameters for the model of Brewin *et al.* [2010] are provided as supporting information Table ts01, for the HPLC data, SFF data, and a combination of HPLC and SFF data in Database A, and for optical depths <2.8 and ≥ 2.8 . Significant differences between model parameters were observed when the model was fitted to HPLC or SFF data in Database A. Differences in model parameters can be related to biases in size-fractionated chlorophyll between SFF and HPLC in Database A, rather than biases in total chlorophyll [see Figures 2b and 3 of Brewin *et al.*, 2014]. In general, C_i^m is higher and S_i lower for the SFF data compared with the HPLC data for both size fractions (Figure 2). Significant differences in C_i^m and S_i are observed when

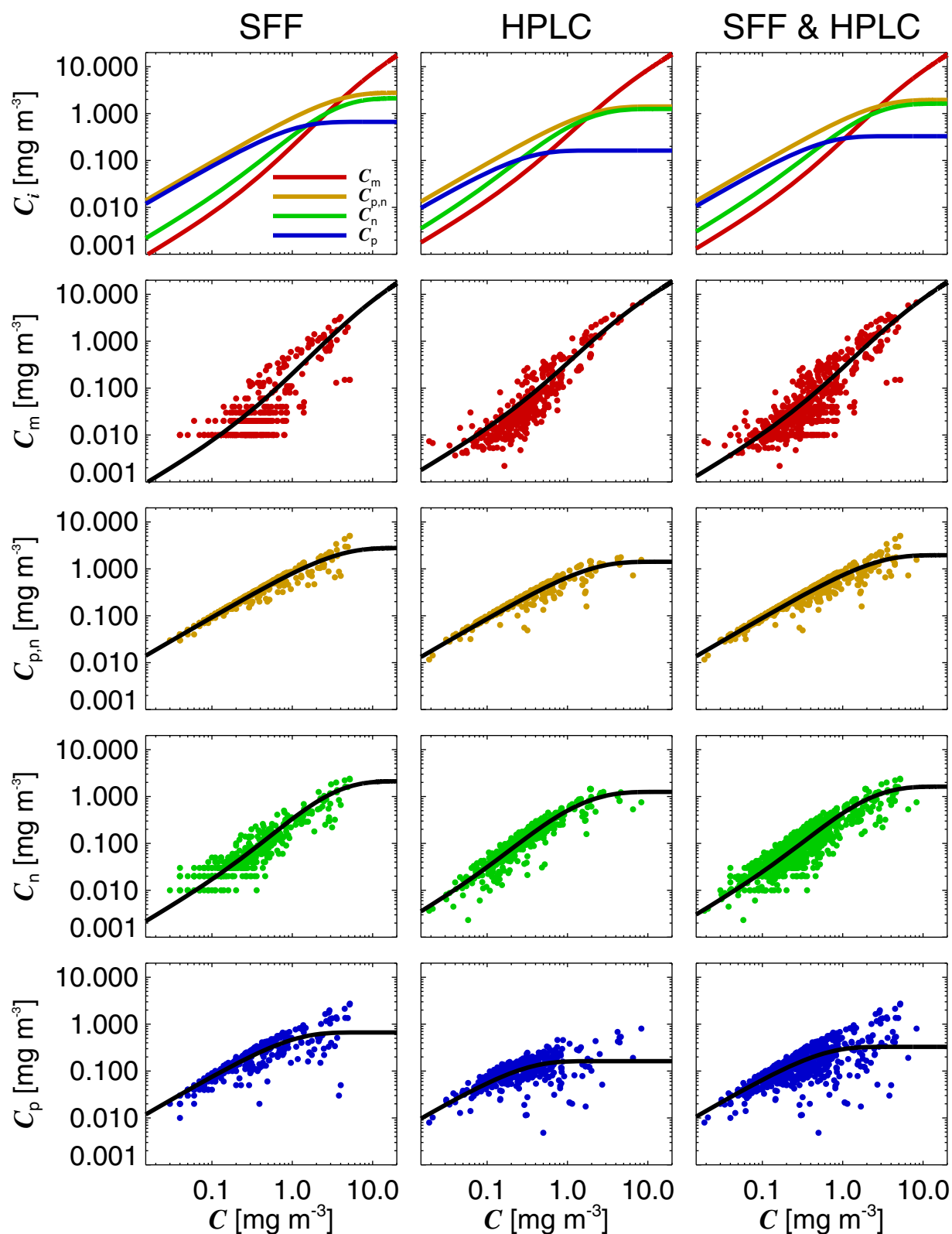


Figure 3. Equation (6) fitted to size-fractionated chlorophyll and total chlorophyll, estimated from HPLC, from fluorometry using size-fractionated filtration (SFF), and both HPLC and SFF.

fitting to HPLC data from <2.8 and ≥ 2.8 optical depths but not for the SFF data, as indicated by overlapping 95% confidence levels for the majority of parameters (supporting information Table ts01). When fitting to a combination of HPLC and SFF data in Database A, 95% confidence levels in the parameters C_i^m and S_i also overlap for data from <2.8 and ≥ 2.8 optical depths (supporting information Table ts01), suggesting no significant variability in model parameters between these two optical layers for this particular data set. Database A was also partitioned into North and South Atlantic samples and the three-component model was fitted to data in the two regions (supporting information Table ts02). Model parameters for each region overlapped at the 95% confidence interval for each in situ methodology (HPLC, SFF, and a combination of both, see supporting information Table ts02), suggesting no significant latitudinal differences in model parameters. Furthermore, no significant differences in model parameters were observed when setting the lower limit of chlorophyll concentration (both size-fractionated and total chlorophyll concentration) on Database A to 0.05 mg m^{-3} .

Figure 2 shows S_i plotted against C_i^m , and D_i plotted against C_i^m for the SFF, HPLC, and combined SFF and HPLC data in Database A. When examining all the fits taken together (HPLC, SFF data, and HPLC & SFF), we observe that the \log_{10} -transformed S_i and \log_{10} -transformed C_i^m are highly negatively correlated ($r = -0.996$, $p = 0.015$). For the $<2 \mu\text{m}$ fraction, D_i and C_i^m are typically lower than for the $<20 \mu\text{m}$ fraction. The parameter D_i is closer to one for the $<20 \mu\text{m}$ fraction (~ 0.94) when compared with the $<2 \mu\text{m}$ fraction (~ 0.72). To simplify the model of *Brewin et al.* [2010], we used the following empirical expression to describe the relationship between D_i and C_i^m ,

$$D_i = \frac{C_i^m - A\{1 - \exp[-(BC_i^m)]\}}{C_i^m}, \quad (5)$$

where A and B are empirical parameters. Equation (5) was fitted to D_i and C_i^m from the SFF, HPLC, and combined SFF and HPLC fits (see Figure 2) and we arrived at values of $A = 0.168$ and $B = 2.412$. Note that this parameterization of equation (5) results in $0.6 \leq D_i \leq 1.0$ (Figure 2), meaning that size-fractionated chlorophyll will never exceed total chlorophyll and that small cells ($<2 \mu\text{m}$ fraction) will always dominate at very low chlorophyll (always $\geq 60\%$ of the chlorophyll biomass). Inserting equation (5) into equation (3) results in the following expression:

$$C_i = C_i^m \left(1 - \exp \left\{ - \frac{[(C_i^m - A\{1 - \exp[-(BC_i^m)])]/C_i^m]}{C_i^m} C \right\} \right). \quad (6)$$

Equation (6) was then fitted to C , $C_{p,nr}$ and C_p derived from the SFF data, from the HPLC data and from a combination of both in Database A, to derive C_i^m , using the same fitting procedure as for equation (3) and setting $A = 0.168$ and $B = 2.412$. Model parameters and results from statistical tests between model and in situ data are provided in Table 2. To further examine how well equation (6) fits data with which it was parameterized, the model is plotted in Figure 3 along with C_m , $C_{p,n}$, C_n , and C_p from Database A as a function of total chlorophyll (C). The model captures the trends in the observations (Figure 3) regardless of whether size-fractionated chlorophyll derived from SFF, HPLC, or a combination of both is used, as indexed by high r values (between 0.648 and 0.972), low Ψ (between 0.093 and 0.262), and δ close to zero (Table 2). Despite equation (6) capturing the trends in both HPLC and SFF data, significant differences are observed in C_i^m between HPLC and SFF data (Table 2), with the C_i^m being higher when fitted to the SFF data for both the $<2 \mu\text{m}$ and $<20 \mu\text{m}$ size fractions.

Interestingly, C_i^m for the $<2 \mu\text{m}$ fraction is always lower than C_i^m for the $<20 \mu\text{m}$ fraction, for HPLC, SFF, or a combination of both in Database A (Table 2). Using HPLC data, *Brewin et al.* [2010, 2011, 2012a, 2012b] and *Brotas et al.* [2013] have observed that, when fitting equation (3) to data sets distributed over different regions of the global ocean, the C_i^m parameter is consistently higher for the $<20 \mu\text{m}$ fraction than for the $<2 \mu\text{m}$ fraction. These results resonate with many other reports from the field: using HPLC data in the Arabian Sea, *Goericke* [2002] observed that when plotting phytoplankton-group-specific chlorophyll concentrations as a function of total chlorophyll, and with the exception of bloom-forming diatoms, most groups reach asymptotic maxima that varied depending on the particular group, with smaller size classes (e.g., cyanobacteria) having lower asymptotic maxima than larger size classes (e.g., Prymnesiophytes). Using size-

Table 2. Parameters of Equation (6) When Fitted to HPLC, Size-Fractionated Filtration (SFF) and a Combination of HPLC and SFF in Database A

Method	Model Parameters ^a		C_p			$C_{p,n}$		
	C_p^m	$C_{p,n}^m$	r	Ψ	δ	r	Ψ	δ
HPLC	0.162 (0.143 ↔ 0.183)	1.416 (1.228 ↔ 1.611)	0.648	0.235	−0.004	0.951	0.113	−0.008
SFF	0.665 (0.552 ↔ 0.800)	2.781 (2.233 ↔ 3.563)	0.865	0.196	0.007	0.972	0.093	−0.002
HPLC & SFF	0.328 (0.288 ↔ 0.370)	1.955 (1.729 ↔ 2.231)	0.723	0.262	0.010	0.959	0.108	−0.004

^aModel parameters are computed as the median of the bootstrap parameter distribution and bracket parameter values refer to the 2.5% and 97.5% confidence intervals on the bootstrap parameter distribution. C_p^m is the asymptotic maximum chlorophyll concentration for picoplankton and $C_{p,n}^m$ the asymptotic maximum chlorophyll concentration for pico-nanoplankton. C_p refers to picoplankton chlorophyll (<2 μm) and $C_{p,n}$ refers to combined pico-nanoplankton chlorophyll (<20 μm).

fractionated fluorometric chlorophyll data in the Mediterranean Sea, *Raimbault et al.* [1988] observed that the total chlorophyll in three size fractions (<1 μm , <3 μm , and <10 μm) have an upper limit (C_i^m), and that this upper limit increases as the size fraction increases from <1 μm to <10 μm . *Riegman et al.* [1993] observed similar relationships in the North Sea for the <3 μm and <8 μm size fractions, and *Gin et al.* [2000] in the eutrophic coastal waters of Singapore for the <1 μm , <5 μm , and <10 μm size fractions (see their Figure 11).

Based on this evidence, and the results in Table 2, we propose that a positive linear relationship exists between C^m and i , such that

$$C^m(i) = \alpha i + \beta, \quad (7)$$

where α describes the slope of the linear relationship and β the intercept. Accordingly, the relationship between the parameter D and i can be expressed as

$$D(i) = \frac{C^m(i) - A\{1 - \exp[-(BC^m(i))]\}}{C^m(i)}. \quad (8)$$

Combining equations (6)–(8) leads to the following expression, describing a multicomponent model of phytoplankton size structure

$$C(i) = C^m(i) \left\{ 1 - \exp \left[-\frac{D(i)}{C^m(i)} C \right] \right\}. \quad (9)$$

Equation (7) was fitted to C^m (Table 2) and i (where i is <2 μm and <20 μm) for the HPLC, SFF, and the combined data sets in Database A (Figure 4) and the parameters are provided in Table 3. Significant differences are observed in α and β when fitted to the HPLC or SFF data sets. The parameter α appears to be in better agreement between the two data sets than the parameter β , and for the HPLC data, the parameter β is close to zero (Table 3). A flow diagram is provided as supporting information Figure fs01 to illustrate the development of the multicomponent model.

4. Results and Discussion

4.1. Model Validation

Database B (Figure 1) was used to test the performance of the multicomponent size model. The model (equation (9)) was applied to the total chlorophyll concentration (C) in Database B, to estimate the size-fractionated concentrations of chlorophyll (C_i) where i is equal to <2 μm , <5 μm , <10 μm , and <20 μm . Considering Database B consisted of SFF data (not HPLC), corresponding parameter values for α and β for the SFF data (Table 3) were used in equations (7)–(9), where $A = 0.168$ and $B = 2.412$. These modeled values were then compared with the measured size-fractionated chlorophyll concentrations derived from Database B. To avoid the undue influence of very small chlorophyll concentrations on the statistical tests, any size-fractionated chlorophyll concentrations (measured or modeled) <0.001 mg m^{-3} were removed (see supporting information Table ts03 for a detailed breakdown of the samples used in Database B). Figure 5 shows the results of this comparison.

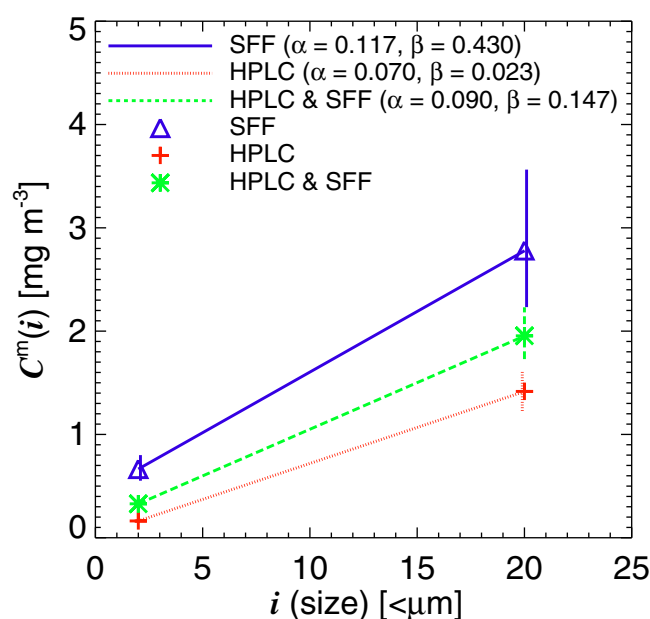


Figure 4. Assumed linear relationship (equation (7)) between C^m and the size fractions using HPLC data, SFF data, and a combination of both.

fractions (Figure 5, $0.628 \leq r \leq 0.871$ and $0.244 \leq \Psi \leq 0.380$), supporting the conceptual framework of the multicomponent model (similar results [not shown] were also obtained when setting the lower limit of chlorophyll in Database B to 0.05 mg m^{-3}). Lower agreement between model and in situ SFF for intermediate size fractions is somewhat expected, considering errors when measuring size-fractionated chlorophyll in situ using SFF (e.g., inaccuracies in pore sizes, filter clogging, and phytoplankton cell breakage) are likely amplified when subtracting one in situ size fraction from another; increasing diversity of phytoplankton communities at intermediate biomass and size ranges [Irigoien *et al.*, 2004; Liu *et al.*, 2009]; and some of the size fractions were not used in the model parameterization.

4.2. Three-Component Model of Brewin *et al.* [2010]

When fitting the three-component model of Brewin *et al.* [2010] to size-fractionated chlorophyll estimated from HPLC and SFF, both approaches yield similar statistical results (Table 2 and supporting information Table ts01), albeit with different parameters. Both HPLC and SFF in Database A appear to support the conceptual framework of the three-component model, in that small cells grow to a given chlorophyll concentration [Sathyendranath *et al.*, 2001], beyond which chlorophyll increases in a given system by the addition of larger size classes of phytoplankton [Raimbault *et al.*, 1988; Yentsch and Phinney, 1989]. Brewin *et al.* [2012b] found that interannual anomalies in phytoplankton size structure, derived using the three-component model and satellite data, were tightly correlated with anomalies in physical variables, consistent with theories on coupling between physical-chemical processes and ecosystem structure, such as those of Margalef [1967, 1978] and Reynolds [1987]. The three-component model has also been supported by flow-cytometry data [Brotas *et al.*, 2013], shown to reflect size-dependent variations in the characteristics of spectral absorption by phytoplankton [Devred *et al.*, 2011; Brewin *et al.*, 2011] and backscattering characteristics

For all the size fractions ($<2 \mu\text{m}$, $<5 \mu\text{m}$, $<10 \mu\text{m}$, and $<20 \mu\text{m}$), the model is in excellent agreement with the in situ data set (Figure 5, $r \geq 0.930$, $\Psi \leq 0.149$, and $\delta \sim 0$). In addition to estimating these size fractions, the model is capable of estimating the chlorophyll concentrations of phytoplankton larger than these size fractions ($>2 \mu\text{m}$, $>5 \mu\text{m}$, $>10 \mu\text{m}$, and $>20 \mu\text{m}$), by subtracting the chlorophyll concentration of the size-fractions ($<2 \mu\text{m}$, $<5 \mu\text{m}$, $<10 \mu\text{m}$, and $<20 \mu\text{m}$) from the total chlorophyll concentration, and capable of estimating intermediate size-fractions (such as $2\text{--}5 \mu\text{m}$, $2\text{--}10 \mu\text{m}$, $5\text{--}10 \mu\text{m}$, and $2\text{--}20 \mu\text{m}$), by subtracting a smaller size fraction (e.g., $<2 \mu\text{m}$) from a large one (e.g., $<5 \mu\text{m}$). The model is seen to be in reasonable agreement with the in situ data for the majority of size

Table 3. Parameters of Equation (7) When Fitted to HPLC, Size-Fractionated Filtration (SFF) and a Combination of HPLC and SFF

Method	Model Parameters ^a	
	α	β
HPLC	0.070 (0.059 \leftrightarrow 0.080)	0.023 (0.001 \leftrightarrow 0.045)
SFF	0.117 (0.091 \leftrightarrow 0.154)	0.430 (0.347 \leftrightarrow 0.519)
HPLC & SFF	0.090 (0.079 \leftrightarrow 0.104)	0.147 (0.114 \leftrightarrow 0.184)

^aModel parameters are computed as the median of the bootstrap parameter distribution and bracket parameter values refer to the 2.5% and 97.5% confidence intervals on the bootstrap parameter distribution.

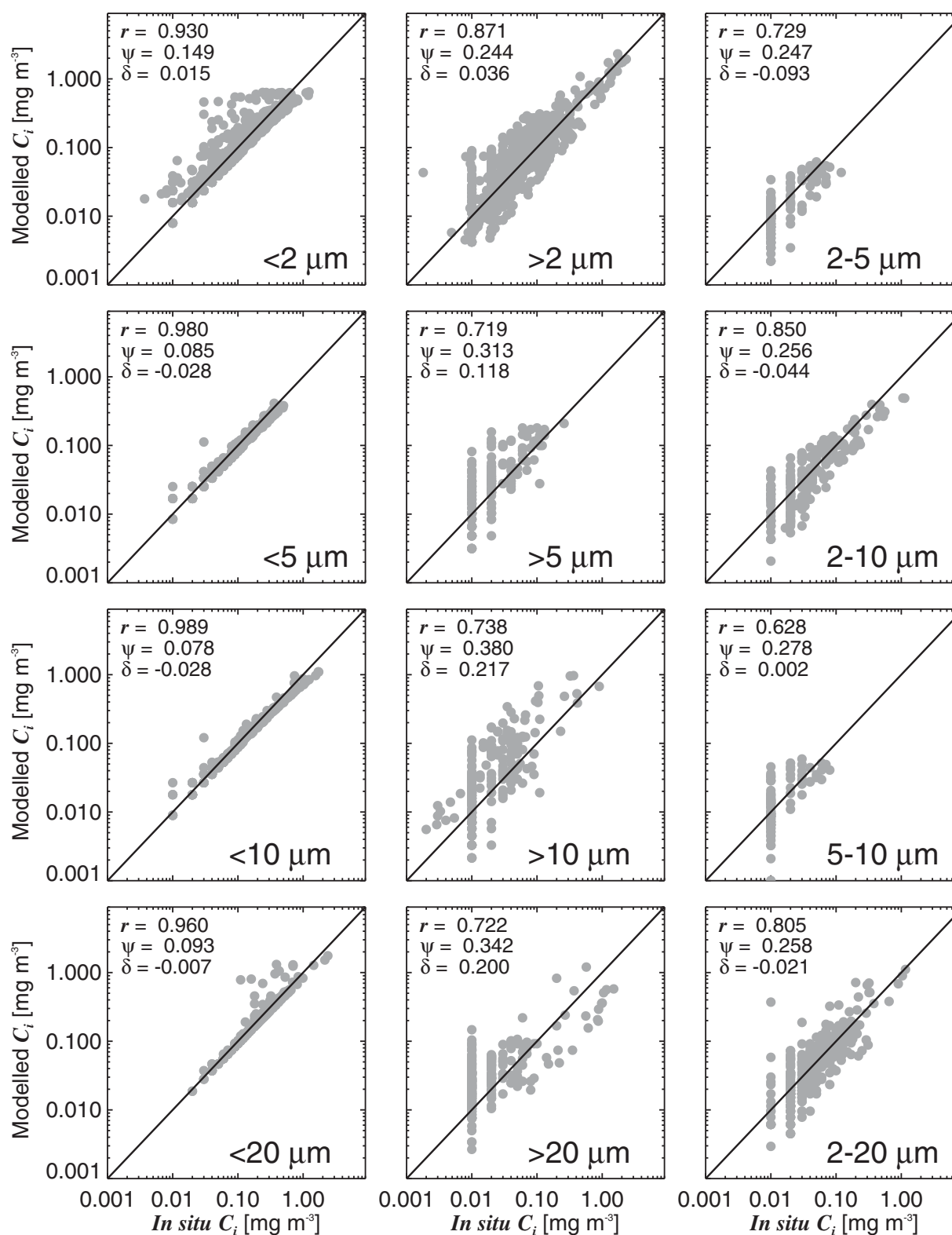


Figure 5. Independent validation of the multicomponent size structure model using different size fractions in Database B (see supporting information Table ts03 for a detailed breakdown of the number of samples used for each size fraction in the statistical tests).

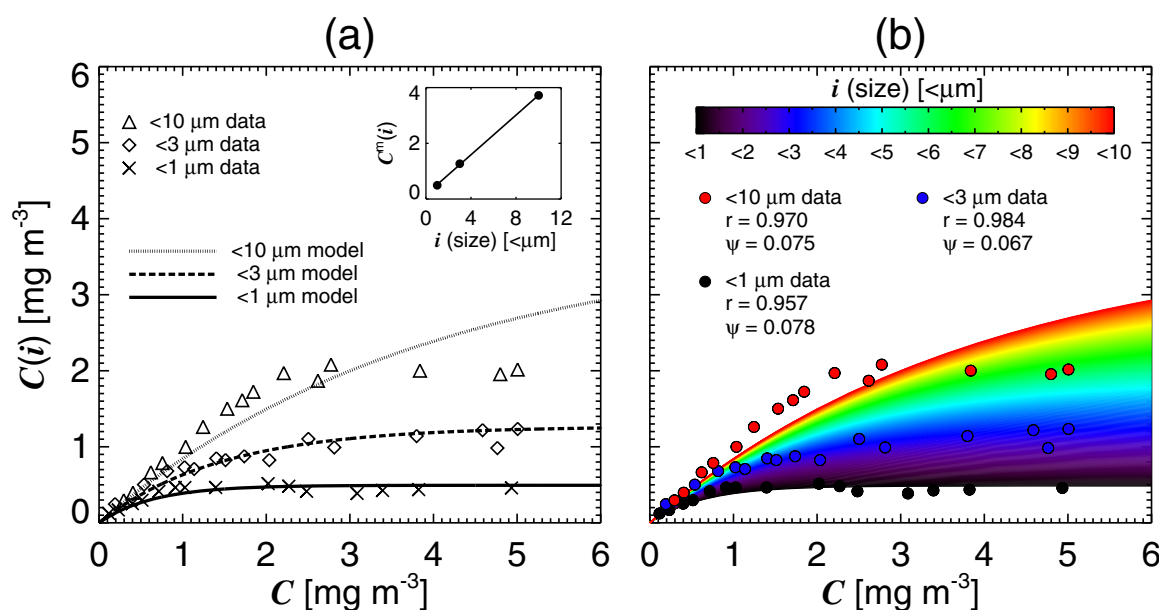


Figure 6. Illustrative example of fitting the multicomponent size structure model to data from Raimbault *et al.* [1988]: (a) data on total chlorophyll and size-fractionated chlorophyll (as <1 μm, <3 μm, and <10 μm) were extracted from Chisholm [1992] using digitizing software and equation (6) was fitted to each size fraction (inset shows C^m derived for each size fraction increasing as a linear function of each size fraction) and (b) based on relationships shown in Figure 6(a), chlorophyll below 10 μm is modeled as a continuous function of size structure and total chlorophyll using equations (7)–(9).

indicative of the different phytoplankton size classes [Brewin *et al.*, 2012a], and complements other SFF data observed in more eutrophic regions [Raimbault *et al.*, 1988; Riegman *et al.*, 1993; Gin *et al.*, 2000]. Marañón *et al.* [2012] recently conducted a meta-analysis of phytoplankton size structure in cold, temperate, and warm waters in the global ocean. In support of the three-component model, they observed that phytoplankton size structure depends strongly on total phytoplankton biomass, and that this dependence occurs irrespective of temperature.

The three-component model is designed to capture the major trends in size structure in the open ocean. Nonetheless, model parameters derived from HPLC data have also been shown to vary between region [Brewin *et al.*, 2012b; Brotas *et al.*, 2013] and to vary between seasons [see Devred *et al.*, 2006]. The parameters of the model are interpretable (C^m corresponds to the maximum chlorophyll concentration a given size class can reach to and S describing the rate of increase in the size-fractionated chlorophyll as a function of the total chlorophyll), such that the approach could be described as “semi-empirical” as opposed to purely “empirical.” However, these model parameters are indicative of ecosystem structure that may change as the marine environment undergoes seasonal and interannual fluctuations. The model is likely to break down in environments that deviate from typical trends, for example in the presence of unusual algal blooms.

The three-component model assumes that the phytoplankton size structure varies with the total phytoplankton chlorophyll biomass. In its current formulation, it does not account for changes in chlorophyll concentration independent of size structure, for example through photoacclimation. When fitting the three-component model to large HPLC databases, model parameters have been observed to change significantly with optical depth [Brewin *et al.*, 2010; Brotas *et al.*, 2013]. However, significant variations in model parameters between two optical layers (<2.8 and ≥2.8 optical depth) were not observed with SFF (or a combination of SFF and HPLC data) in Database A used in this study (supporting information Table ts01). This may be in part because Database A is smaller when compared with HPLC data used in the Brewin *et al.* [2010] and the Brotas *et al.* [2013] studies, or perhaps (as an artifact) Database A is less evenly distributed over the photic range (predominately in oligotrophic waters). Nonetheless, depth variations in model parameters reported by Brewin *et al.* [2010] and Brotas *et al.* [2013] may in part be a result of the reductionist character of the HPLC-pigment-to-size-class approach. We note in particular that (i) photoprotective carotenoids (e.g., zeaxanthin and alloxanthin) used in the HPLC approach may vary with depth independently of phytoplankton size structure; (ii) there may be depth-dependent variations in the specific pigments

attributed to each size class proposed by *Vidussi et al.* [2001] and in the multiple regression coefficients proposed by *Uitz et al.* [2006] to infer the chlorophyll *a* concentration from the diagnostic pigments; and (iii) there could be a possible effect of depth-dependent variations in ecotypes of picoplankton [*Bouman et al.*, 2000; *Veldhuis et al.*, 2005; *Kulk et al.*, 2011] on the HPLC-pigment-to-size-class relationships. Additional depth-resolved in situ data are required to ascertain the conditions under which the parameters of three-component model vary with optical depth. This may include an assessment of the influence of variations in incident irradiance on model parameters, to integrate any influence of photoacclimation.

4.3. Multicomponent Model of Phytoplankton Size Structure

By making two simple assumptions (empirically relating the parameter S to the parameter C^m and letting $C^m(i)$ increase linearly with size i) the three-component model was extended into a multicomponent model of size structure (equations (7)–(9)). When verified with independent data (Database B), the model performed reasonably well at deriving different size fractions (Figure 5), especially when considering only the $<2\ \mu\text{m}$ and $<20\ \mu\text{m}$ size fractions were used in the model parameterization. Figure 6a provides an example of fitting equation (6) using data from *Raimbault et al.* [1988] in the Mediterranean Sea, extracted digitally from *Chisholm* [1992], at the $<1\ \mu\text{m}$, $<3\ \mu\text{m}$, and $<10\ \mu\text{m}$ size fractions and setting $A = 0.168$ and $B = 2.412$. As illustrated in the inset of Figure 6a, the derived parameter C^m is observed to increase linearly with increasing size fraction (equation (7), $\alpha = 0.164$ and $\beta = 0.356$). The multicomponent model (equation (8)) is further illustrated in Figure 6b. It can be seen that as the size fraction increases from $<1\ \mu\text{m}$ to $<10\ \mu\text{m}$, the upper limit on chlorophyll (C^m) increases, and beyond this threshold, chlorophyll increases only by the addition of larger size classes of phytoplankton.

The advantage of the multicomponent model is that for the same number of parameters, it is no longer constrained to three size classes. Akin to the approach of *Kostadinov et al.* [2009] for deriving particle volume concentrations for different size fractions from backscattering data, size diameter limits can be chosen a priori, allowing users to define the specific size fractions of interest. The multicomponent model would be preferable in use over the three-component model when a user is interested in a specific size fraction that does not fit the pico-, nano-, or micro-size range ($<2\ \mu\text{m}$, $2\text{--}20\ \mu\text{m}$, or $>20\ \mu\text{m}$). Nonetheless, the multicomponent model is applicable only to the size range for which it was parameterized (i.e., the minimum and maximum value for i in the parameter $C^m(i)$ is 2 and $20\ \mu\text{m}$, respectively).

Parameters for the multicomponent model were provided for HPLC, SFF data, and a combination of both. The parameter α was found to be in reasonable agreement between the various methods (Table 3). However, the parameter β was considerably different. The two in situ methods (HPLC and SFF) have advantages and disadvantages. SFF data explicitly partition the size classes, but difficulties arise from inaccuracies in pore sizes, filter clogging, and phytoplankton cell breakage [*Droppo*, 2000]. Whereas the method of *Welschmeyer* [1994] was used in the determination of chlorophyll *a* fluorometrically, which minimizes the influence of chlorophyll *b*, chlorophyll *c*₂, and pheopigments on chlorophyll *a* estimates, it is possible that this influence varies depending on the size fraction of interest, especially when considering chlorophyll *b* is likely present in higher concentrations in the smaller size classes [*Vidussi et al.*, 2001; *Uitz et al.*, 2006] and at the deep chlorophyll maximum [*Barlow et al.*, 2002]. HPLC is appealing for assessing large-scale patterns in size structure given the vast amount of data, but it does not strictly reflect the true size of phytoplankton [*Vidussi et al.*, 2001; *Uitz et al.*, 2006]. As the size structure (i) tends to zero, it would be expected that $C^m(i)$ also tends to zero, such that a β parameter close to zero would appear more realistic, as in the case of the HPLC approach (Table 3). Nonetheless, further work is required to ascertain uncertainty when inferring size structure from HPLC and SFF [*Brewin et al.*, 2014].

4.4. Theoretical Comparison of the Multicomponent Model With a Size Spectrum Model

The multicomponent model may be compared with other phytoplankton size spectrum models. *Platt and Denman* [1977] proposed a normalized biomass size spectrum that relates the fraction of total biomass contained in a given size class, normalized by the width of that size class, with the size of the size class, using a power law dependence, such that

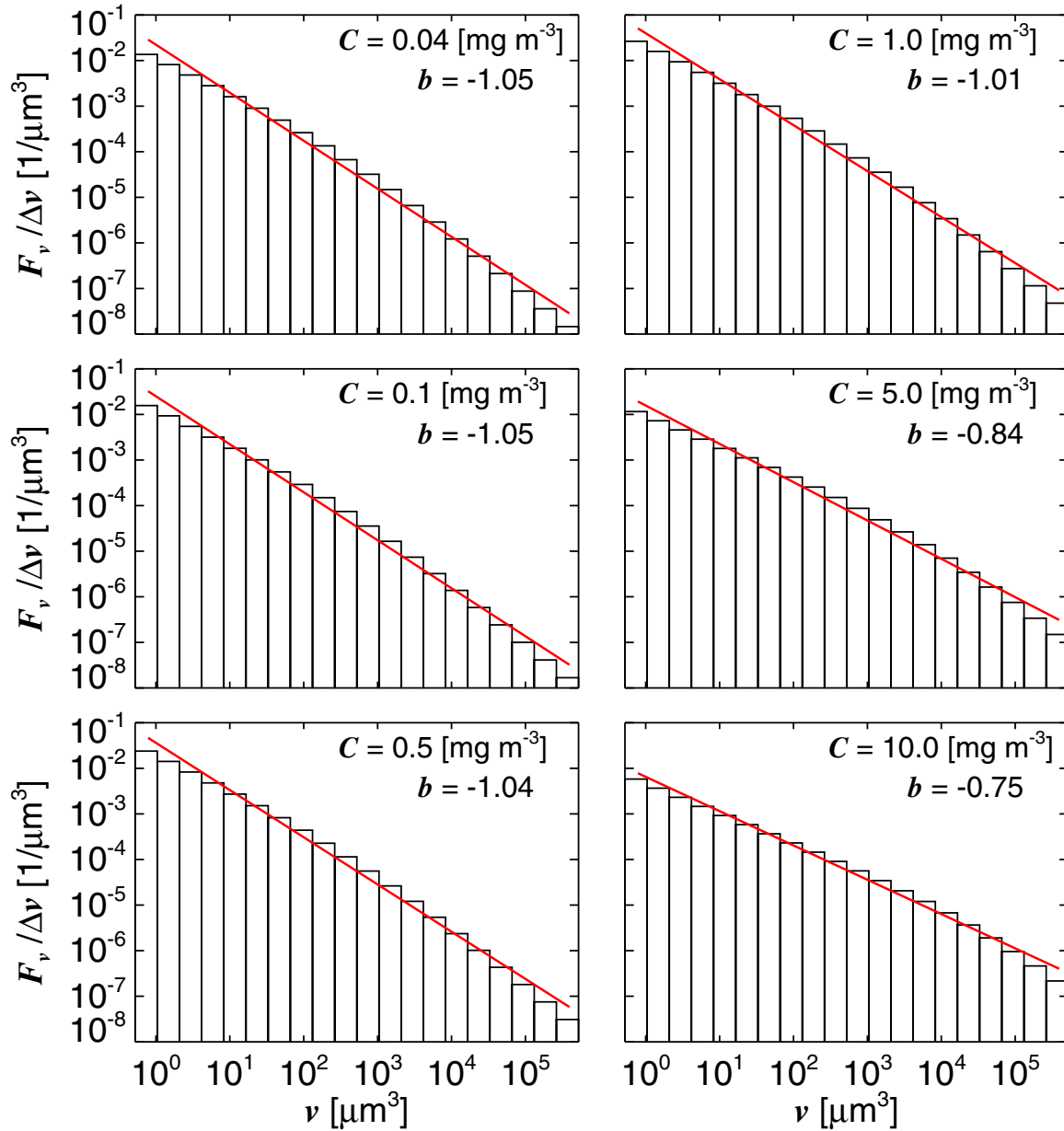


Figure 7. Normalized biomass size-spectra computed using the multicomponent model for a variety of total chlorophyll concentrations (C).

$$\frac{F_v}{\Delta v} = a v^b, \quad (10)$$

where v is the size class, Δv refers to the size class interval, the fraction of total biomass residing in a given size class is taken here as the chlorophyll concentration within the size class divided by total chlorophyll and is denoted (F_v), and a and b are constants, the latter referring to the exponent of the size spectrum. Using the multicomponent model, the normalized biomass within a given size class can be computed according to

$$\frac{F_v}{\Delta v} = \frac{\left(\left\{ C^m(i_2) \left(1 - \exp \left[-\frac{D(i_2)}{C^m(i_2)} C \right] \right) \right\} - \left\{ C^m(i_1) \left(1 - \exp \left[-\frac{D(i_1)}{C^m(i_1)} C \right] \right) \right\} \right) / C}{\frac{\pi}{6} I_2^3 - \frac{\pi}{6} I_1^3}, \quad (11)$$

where i_1 and i_2 are the lower and upper diameter of the phytoplankton size class interval, such that $\Delta v = (\pi/6)i_2^3 - (\pi/6)i_1^3$ and $v = [(\pi/6)i_2^3 + (\pi/6)i_1^3]/2$. According to equation (11), the normalized biomass size spectrum can be computed as a function of chlorophyll (C).

To compare the multicomponent model with a size spectrum model, the normalized biomass was estimated for 20 logarithmically spaced bins (base 10) between 1 and 100 μm , using the SFF parameters (Table 3). The minimum and maximum value for i in the multicomponent model is currently set as 2 and 20 μm ; however, we extended this range to 1 and 100 μm for this theoretical comparison so as to better capture the typical phytoplankton size range. Figure 7 shows plots of the normalized biomass size spectrum ($F_v/\Delta v$) computed using equation (11) as a function of the size class (v) for a variety of chlorophyll concentrations (C) ranging from 0.04 to 10.0 mg m^{-3} . The normalized biomass estimated from the multicomponent model exhibits a power law dependence on cell size, consistent with previous observations [Sheldon *et al.*, 1972; Platt and Denman, 1977; Peters, 1983; Roy *et al.*, 2011]. When fitting a power law model (equation (10)) to the normalized biomass spectra computed using the multicomponent model, for the size range to 1 and 100 μm (Figure 7), the exponent of the size spectrum (b) varied between -1.05 and -0.75 , with b values ranging from -1.05 to -1.01 for chlorophyll concentrations from 0.04 to 1.0 mg m^{-3} , with the slope increasing to -0.84 and -0.75 at 5.0 and 10.0 mg m^{-3} , respectively. This flattening of the exponent of the size spectrum (b) from oligotrophic to eutrophic waters is consistent with previous literature [e.g., Kostadinov *et al.*, 2009], and the values for b estimated using the multicomponent model are consistent with those estimated independently using AMT cruises 12, 13, and 14 [San Martin *et al.*, 2006] and in other oligotrophic waters [Quinones *et al.*, 2003].

4.5. The Asymptotic Maximum

The multicomponent model assumes an upper limit or asymptotic maximum to the different size fractions (C^m) which increases with phytoplankton size (i). This is supported by a number of independent studies using HPLC and size-fractionated chlorophyll data in a variety of marine environments [Raimbault *et al.*, 1988; Chisholm, 1992; Riegman *et al.*, 1993; Gin *et al.*, 2000; Goericke, 2002]. In this section, we attempt to interpret the biological significance of this parameter, by exploring possible explanations for such an upper limit, including bottom-up or top-down processes, or a combination of both.

Gin *et al.* [2000] postulated that an upper limit to the different size classes lies in the metabolic constraints of size. Thingstad and Sakshaug [1990] found that as nutrient concentrations increase, under constant light intensity, the growth rate of a particular size class of phytoplankton increases until eventually some maximum is reached according to Michaelis-Menten kinetics (or alternatively a Holling type 2 functional response). Gin *et al.* [2000] suggest that, as maximum growth rates are known to be inversely related to size [Eppey and Sloan, 1966; Schlesinger *et al.*, 1981; Peters, 1983; Geider *et al.*, 1986], once the growth rates of small cells are saturated, ambient nutrient concentrations can increase enough to allow larger phytoplankton, which generally have larger half-saturation constants [e.g., Aksnes and Egge, 1991], to grow. They concluded that the bottom-up hypothesis offers an explanation for the upper limit and that phytoplankton communities are structured in response to nutrient input. However, when light is not limiting, nutrient availability during the day at a specific location may not always be a controlling factor for some larger species. For instance, some dinoflagellates are motile and have been known to use diel vertical migration to acquire nutrients [Cullen and Horrigan, 1981; Cullen, 1985].

Loss terms (e.g., grazing and viral lysis) may also impose an upper limit on size fractions. There is evidence that marine viruses can control phytoplankton communities and resource allocation [Bratbak *et al.*, 1993; Mann, 2003; Bailey *et al.*, 2004; Zeng and Chisholm, 2012], possibly influencing the observed upper limits of the different size fractions. Consistent with the concept of the multicomponent model, Goericke [2002] observed that some phytoplankton communities in the High-Nutrient-Low-Chlorophyll areas of the monsoonal Arabian Sea have constrained biomass thresholds (C^m). Based on in situ data and incubation experiments, Goericke [2002] concluded that in the Arabian Sea the phytoplankton community structure is controlled by top-down processes (grazers), rather than bottom-up processes (nutrients), through the grazing by mesozooplankton on diatoms and the grazing by microzooplankton on smaller cells. Riegman *et al.* [1993] also provide evidence from in situ and dilution experiments that high growth rates of microzooplankton make smaller algae susceptible to grazing control, and that due to their size, larger algae are less susceptible to microzooplankton predation. According to this top-down concept, the maximum biomass of

small cells (C^m) is controlled by grazing of microzooplankton, and once this is reached, remaining nutrients and/or light energy can be transformed into biomass of the next size class. Although the biomass of larger cells ($>20\ \mu\text{m}$) provides forage for mesozooplankton, it is controlled mainly by the level of nutrients, light and sedimentation, as opposed to grazing, especially given the slower response of mesozooplankton to an increase in food availability.

There is also some evidence to suggest that the asymptotic maximum of the different size fractions may be controlled by environmental factors. Growth rates of phytoplankton and zooplankton are correlated with environmental variables such as temperature [McLaren, 1963; Eppley, 1972; Raven and Geider, 1988; Bouman *et al.*, 2005], thus likely to influence the bottom-up and top-down processes described above and possibly contribute to the assembly of phytoplankton communities at large scales [Li *et al.*, 2006]. Nonetheless, the relationship between temperature and size structure may be an artifact of a general inverse relationship between temperature and nutrient supply [Agawin *et al.*, 2000]. Marañón *et al.* [2012] concluded that resource availability (e.g., nutrients and light) irrespective of temperature is the key factor explaining the relative success of different algal size classes. Sathyendranath and Platt [2007] examined the potential role of the spectral quality of the underwater light field in modulating species succession in the ocean. As the size of the phytoplankton cell increases, the magnitude of the blue peak of the phytoplankton specific absorption coefficient decreases [Sathyendranath *et al.*, 2001; Ciotti *et al.*, 2002; Devred *et al.*, 2006; Uitz *et al.*, 2008; Nair *et al.*, 2008; Brewin *et al.*, 2011]. Through simple model calculations, Sathyendranath and Platt [2007] concluded that, based on the spectral characteristics of different phytoplankton communities, smaller cells (e.g., *Prochlorococcus*) are likely to out-perform other phytoplankton groups in clear, blue, oligotrophic waters, and large cells (e.g., diatoms) in greener eutrophic waters. Thus, the asymptotic maximum observed for the different size fractions may, in part, be controlled by changes in the spectral characteristics of phytoplankton with size and the influence of phytoplankton on the spectral quality of the underwater light field.

One possible way to unravel the causes of the observed asymptotic maxima for the different size fractions is through more mechanistic multiphytoplankton biogeochemical models. Ward *et al.* [2012] have developed a size-structured food-web model, embedded in a global ocean circulation model, based on observed physiological and ecological properties of marine organisms that are related to cell size. Their model was found to reproduce not only global distributions of nutrients, biomass, and primary productivity but also phytoplankton size structure. Model simulations showed that as the total biomass increases, the biomass within individual size classes begins to saturate, first in the smallest size classes then in larger size classes, a result consistent with the multicomponent model presented here. Determining key mechanisms controlling the asymptotic maximum to the different size fractions will ultimately lead to further model improvement.

5. Summary

Using 1445 size-fractionated fluorometric chlorophyll (SFF) measurements taken over a 17 year period along the Atlantic Meridional Transect, we extended the three-component model of Brewin *et al.* [2010] into a multicomponent model of phytoplankton size structure. The three-component model was fitted to both the HPLC and SFF size-fractionated chlorophyll data yielding reasonable fits for both data sets but with different parameters. Despite these differences, both HPLC and SFF data support the conceptual framework on which the three-component model is based, such that the abundance of small cells increases to a given chlorophyll concentration beyond which chlorophyll may increase only by the addition of larger celled phytoplankton, suggesting consistency between HPLC and SFF derived size-fractionated chlorophyll.

By relating the parameters of the model empirically, and assuming the maximum chlorophyll concentration to which cells grow to increases linearly with cell size, the three-component model was extended into a multicomponent model of phytoplankton size structure. This has the advantage that, for the same number of parameters, the model was no longer constrained to three size classes. The model was verified with 1037 independent measurements of SFF at a variety of size fractions and found to perform well. We envisage that the model will be a useful tool for studying the assembly of phytoplankton size structure at large scales; evaluating emergent properties of size-structure-based biogeochemical models; assimilating information on size structure into biogeochemical models; and understanding the influence of size structure on

primary production, export production, food-web models and their implications for the marine ecosystem under climatic change.

Acknowledgments

We thank the officers and crew of RRS James Clark Ross and RRS Discovery, all scientists who helped in the acquisition and analyses of AMT data, especially Jim Aiken, Ray Barlow, Emilio Marañón, Emilio Fernández, Alex Poulton, Claire Widdicombe, and Gerald Moore. We also thank Rob Thomas from the British Oceanographic Database Centre (BODC) and two anonymous reviewers for their useful suggestions during the review process. Data used in this publication are available through the BODC. This work is supported by a grant from the Changing Earth Science Network initiative funded by the STSE program of the European Space Agency (ESA), by the UK National Centre for Earth Observation and by the Ocean Colour Climate Change Initiative of ESA. This study is a contribution to the international IMBER project and was supported by the UK Natural Environment Research Council National Capability funding to Plymouth Marine Laboratory and the National Oceanography Centre, Southampton. This is contribution number 249 of the AMT programme and dedicated to the memory of Hazel Brewin.

References

- Agawin, N. S. R., C. M. Duarte, and S. Agustí (2000), Nutrient and temperature control of the contribution of picoplankton to phytoplankton biomass and production, *Limnol. Oceanogr.*, **45**, 591–600, doi:10.4319/lo.2000.45.3.0591.
- Aiken, J., J. R. Fishwick, S. Lavender, R. Barlow, G. F. Moore, H. Sessions, S. Bernard, J. Ras, and N. J. Hardman-Mountford (2007), Validation of MERIS reflectance and chlorophyll during the BENCAL cruise October 2002: Preliminary validation of new demonstration products for phytoplankton functional types and photosynthetic parameters, *Int. J. Remote Sens.*, **28**(3–4), 497–516, doi:10.1080/01431160600821036.
- Aiken, J., N. J. Hardman-Mountford, R. Barlow, J. Fishwick, T. Hirata, and T. Smyth (2008), Functional links between bioenergetics and bio-optical traits of phytoplankton taxonomic groups: An overarching hypothesis with applications for ocean colour remote sensing, *J. Plankton Res.*, **30**(2), 165–181, doi:10.1093/plankt/fbm098.
- Aiken, J., Y. Pradhan, R. Barlow, S. Lavender, A. Poulton, P. Holligan, and N. J. Hardman-Mountford (2009), Phytoplankton pigments and functional types in the Atlantic Ocean: A decadal assessment, 1995–2005, *Deep Sea Res., Part II*, **56**, 899–917, doi:10.1016/j.dsr2.2008.09.017.
- Aksnes, D. L., and J. K. Egge (1991), A theoretical model for nutrient uptake in phytoplankton, *Mar. Ecol. Prog. Ser.*, **70**, 65–72.
- Aumont, O., E. Maier-Reimer, S. Blain, and P. Monfray (2003), An ecosystem model of the global ocean including Fe, Si, P colimitations, *Global Biogeochem. Cycles*, **17**(2), 1060, doi:10.1029/2001GB001745.
- Bailey, S., M. R. J. Clokie, A. Millard, and N. H. Mann (2004), Cyanophage infection and photoinhibition in marine cyanobacteria, *Res. Microbiol.*, **155**, 720–725, doi:10.1016/j.resmic.2004.06.002.
- Barlow, R., D. G. Cummings, and S. W. Gibb (1997), Improved resolution of mono- and divinyl Chlorophylls *a* and *b* and Zeaxanthin and Lutein in phytoplankton extracts using reverse phase C-8 HPLC, *Mar. Ecol. Prog. Ser.*, **161**, 303–307, doi:10.3354/meps161303.
- Barlow, R. G., J. Aiken, P. M. Holligan, D. G. Cummings, S. Mariotena, and S. Hooker (2002), Phytoplankton pigment and absorption characteristics along meridional transects in the Atlantic Ocean, *Deep Sea Res., Part I*, **49**, 637–660, doi:10.1016/S0967-0637(01)00081-4.
- Barlow, R. G., J. Aiken, G. F. Moore, P. M. Holligan, and S. Lavender (2004), Pigment adaptations in surface phytoplankton along the eastern boundary of the Atlantic Ocean, *Mar. Ecol. Prog. Ser.*, **281**, 13–26, doi:10.3354/meps281013.
- Blackford, J. C., J. I. Allen, and F. J. Gilbert (2004), Ecosystem dynamics at six contrasting sites: A generic modelling study, *J. Mar. Syst.*, **52**(1–4), 191–215, doi:10.1016/j.jmarsys.2004.02.004.
- Blanchard, J. L., S. Jennings, R. Holmes, J. Harle, G. Merino, J. I. Allen, J. Holt, N. K. Dulvy, and M. Barange (2012), Potential consequences of climate change for primary production and fish production in large marine ecosystems, *Philos. Trans. R. Soc. B*, **367**(1605), 2979–2989, doi:10.1098/rstb.2012.0231.
- Bouman, H., T. Platt, S. Sathyendranath, and V. Stuart (2005), Dependence of light-saturated photosynthesis on temperature and community structure, *Deep Sea Res., Part I*, **52**, 1284–1299, doi:10.1016/j.dsr.2005.01.008.
- Bouman, H. A., T. Platt, G. W. Kraay, S. Sathyendranath, and B. D. Irwin (2000), Bio-optical properties of the subtropical North Atlantic. I. Vertical variability, *Mar. Ecol. Prog. Ser.*, **200**, 3–18, doi:10.3354/meps200003.
- Boyd, P. W., and P. Newton (1999), Does planktonic community structure determine downward particulate organic carbon flux in different oceanic provinces?, *Deep Sea Res., Part I*, **46**, 63–91, doi:10.1016/S0967-0637(98)00066-1.
- Bratbak, G., J. K. Egge, and M. Heldal (1993), Viral mortality of the marine alga *Emiliania huxleyi* (Haptophyceae) and termination of algal blooms, *Mar. Ecol. Prog. Ser.*, **93**, 39–48.
- Brewin, R. J. W., S. Sathyendranath, T. Hirata, S. J. Lavender, R. Barciela, and N. J. Hardman-Mountford (2010), A three-component model of phytoplankton size class for the Atlantic Ocean, *Ecol. Modell.*, **221**, 1472–1483, doi:10.1016/j.ecolmodel.2010.02.014.
- Brewin, R. J. W., E. Devred, S. Sathyendranath, S. J. Lavender, and N. J. Hardman-Mountford (2011), Model of phytoplankton absorption based on three size classes, *Appl. Opt.*, **50**(2), 4535–4549, doi:10.1364/AO.50.004535.
- Brewin, R. J. W., G. Dall'Olmo, S. Sathyendranath, and N. J. Hardman-Mountford (2012a), Particle backscattering as a function of chlorophyll and phytoplankton size structure in the open-ocean, *Opt. Express*, **20**, 17,632–17,652, doi:10.1364/OE.20.017632.
- Brewin, R. J. W., T. Hirata, N. J. Hardman-Mountford, S. Lavender, S. Sathyendranath, and R. Barlow (2012b), The influence of the Indian Ocean Dipole on interannual variations in phytoplankton size structure as revealed by Earth Observation, *Deep Sea Res., Part II*, **77–80**, 117–127, doi:10.1016/j.dsr2.2012.04.009.
- Brewin, R. J. W., S. Sathyendranath, P. K. Lange, and G. Tilstone (2014), Comparison of two methods to derive the size-structure of natural populations of phytoplankton, *Deep Sea Res., Part I*, **85**, 72–79, doi:10.1016/j.dsr.2013.11.007.
- Bricaud, A., H. Claustre, J. Ras, and K. Oubelkheir (2004), Natural variability of phytoplanktonic absorption in oceanic waters: Influence of the size structure of algal populations, *J. Geophys. Res.*, **109**, C11010, doi:10.1029/2004JC002419.
- Bricaud, A., A. M. Ciotti, and B. Gentili (2012), Spatial-temporal variations in phytoplankton size and colored detrital matter absorption at global and regional scales, as derived from twelve years of SeaWiFS data (1998–2009), *Global Biogeochem. Cycles*, **26**, GB1010, doi:10.1029/2010GB003952.
- Briggs, N., M. J. P. Perry, I. Cetinić, C. Lee, E. D'Asaro, A. M. Gray, and E. Rehm (2011), High-resolution observations of aggregate flux during a sub-polar North Atlantic spring bloom, *Deep Sea Res., Part I*, **58**, 1031–1039, doi:10.1016/j.dsr.2011.07.007.
- Brotas, V., et al. (2013), Deriving phytoplankton size classes from satellite data: Validation along a trophic gradient in the eastern Atlantic Ocean, *Remote Sens. Environ.*, **134**, 66–77, doi:10.1016/j.rse.2013.02.013.
- Campbell, J. W. (1995), The lognormal distribution as a model for bio-optical variability in the sea, *J. Geophys. Res.*, **100**(C7), 13,237–13,254, doi:10.1029/95JC00458.
- Chisholm, S. W. (1992), Phytoplankton size, in *Primary Productivity and Biogeochemical Cycles in the Sea*, edited by P. G. Falkowski and A. D. Woodhead, pp. 213–237, Springer, N. Y.
- Ciotti, A. M., and A. Bricaud (2006), Retrievals of a size parameter for phytoplankton and spectral light absorption by coloured detrital matter from water-leaving radiances at SeaWiFS channels in a continental shelf off Brazil, *Limnol. Oceanogr. Methods*, **4**, 237–253, doi:10.4319/lom.2006.4.237.
- Ciotti, A. M., J. J. Cullen, and M. R. Lewis (1999), A semi-analytical model of the influence of phytoplankton community structure on the relationship between light attenuation and ocean color, *J. Geophys. Res.*, **104**, 1559–1578, doi:10.1029/1998JC900021.

- Ciotti, A. M., M. R. Lewis, and J. J. Cullen (2002), Assessment of the relationships between dominant cell size in natural phytoplankton communities and the spectral shape of the absorption coefficient, *Limnol. Oceanogr.*, **47**(2), 404–417, doi:10.4319/lo.2002.47.2.0404.
- Claustre, H., M. Babin, D. Merien, J. Ras, L. Prieur, and S. Dallot (2005), Toward a taxon-specific parameterization of bio-optical models of primary production: A case study in the North Atlantic, *J. Geophys. Res.*, **110**, C07S12, doi:10.1029/2004JC002634.
- Cullen, J. J. (1985), Diel vertical migration by dinoflagellates: Roles of carbohydrate metabolism and behavioral flexibility, *Contrib. Mar. Sci.*, **27**, 135–152.
- Cullen, J. J., and S. G. Horrigan (1981), Effects of nitrate on the diurnal vertical migration, carbon to nitrogen ratio, and the photosynthetic capacity of the dinoflagellate *Gymnodinium splendens*, *Mar. Biol.*, **62**, 81–89.
- Devred, E., S. Sathyendranath, V. Stuart, H. Maas, O. Ulloa, and T. Platt (2006), A two-component model of phytoplankton absorption in the open ocean: Theory and applications, *J. Geophys. Res.*, **111**, C03011, doi:10.1029/2005JC002880.
- Devred, E., S. Sathyendranath, V. Stuart, and T. Platt (2011), A three component classification of phytoplankton absorption spectra: Applications to ocean-colour data, *Remote Sens. Environ.*, **115**(9), 2255–2266, doi:10.1016/j.rse.2011.04.025.
- Droppo, I. G. (2000), Filtration in particle size analysis, in *Encyclopedia of Analytical Chemistry*, edited by R. A. Meyers, pp. 5397–5413, John Wiley, Chichester, U. K.
- Efron, B. (1979), Bootstrap methods: Another look at the jackknife, *Ann. Stat.*, **7**, 1–26.
- Eppley, R. W. (1972), Temperature and phytoplankton growth in the sea, *Fish. Bull.*, **70**(4), 1063–1085.
- Eppley, R. W., and B. J. Peterson (1979), Particulate organic matter flux and planktonic new production in the deep ocean, *Nature*, **282**, 677–680, doi:10.1038/282677a0.
- Eppley, R. W., and P. R. Sloan (1966), Growth rates of marine phytoplankton: Correlation with light absorption by cell chlorophyll-*a*, *Physiol. Plantarum*, **19**, 47–49.
- Fujiwara, M., T. Hirawake, K. Suzuki, and S.-I. Saitoh (2011), Remote sensing of size structure of phytoplankton communities using optical properties of the Chukchi and Bering Sea shelf region, *Biogeosciences*, **4**, 817–835, doi:10.5194/bg-8-3567-2011.
- Geider, R. J., T. Platt, and J. A. Raven (1986), Size dependence of growth and photosynthesis in diatoms: A synthesis, *Mar. Ecol. Prog. Ser.*, **30**, 93–104.
- Gibb, S. W., R. G. Barlow, D. G. Cummings, N. W. Rees, C. C. Trees, P. M. Holligan, and D. Suggett (2000), Surface phytoplankton pigment distributions in the Atlantic Ocean: An assessment of basin scale variability between 50°N and 50°S, *Prog. Oceanogr.*, **45**, 339–368, doi:10.1016/S0079-6611(00)00007-0.
- Gin, K. Y.-H., X. Lin, and S. Zhang (2000), Dynamics and size structure of phytoplankton in the coastal waters of Singapore, *J. Plankton Res.*, **22**(8), 1465–1484, doi:10.1093/plankt/22.8.1465.
- Goericke, R. (2002), Top-down control of phytoplankton biomass and community structure in the monsoonal Arabian sea, *Limnol. Oceanogr.*, **47**(5), 1307–1323, doi:10.4319/lo.2002.47.5.1307.
- Guidi, L., L. Stemmann, G. A. Jackson, F. Ibanez, H. Claustre, L. Legendre, M. Picheral, and G. Gorsky (2009), Effects of phytoplankton community on production, size and export of large aggregates: A world-ocean analysis, *Limnol. Oceanogr.*, **54**(6), 1951–1963, doi:10.4319/lo.2009.54.6.1951.
- Hirata, T., J. Aiken, N. J. Hardman-Mountford, T. J. Smyth, and R. G. Barlow (2008), An absorption model to derive phytoplankton size classes from satellite ocean colour, *Remote Sens. Environ.*, **112**(6), 3153–3159, doi:10.1016/j.rse.2008.03.011.
- Hirata, T., et al. (2011), Synoptic relationships between surface chlorophyll-*a* and diagnostic pigments specific to phytoplankton functional types, *Biogeosciences*, **8**, 311–327, doi:10.5194/bg-8-311-2011.
- Hirata, T., S. Saux-Picart, T. Hashioka, M. Aita-Noguchi, H. Sumata, M. Shigemitsu, J. I. Allen, and Y. Yamanaka (2013), A comparison between phytoplankton community structures derived from a global 3D ecosystem model and satellite observation, *J. Mar. Syst.*, **109**–110, 129–137, doi:10.1016/j.jmarsys.2012.01.009.
- Irigoin, X., J. Huisman, and R. P. Harris (2004), Global biodiversity patterns of marine phytoplankton and zooplankton, *Nature*, **429**, 863–867, doi:10.1038/nature02593.
- Jeffrey, S. W., and R. F. C. Mantoura (1997), Development of pigment methods for oceanography: SCOR-supported working groups and objectives, in *Phytoplankton Pigments in Oceanography: Guidelines to Modern Methods*, edited by S. W. Jeffrey, R. F. C. Mantoura, and S. W. Wright, pp. 38–84, UNESCO Publishing, Paris.
- Kishi, M. J., et al. (2007), NEMURO—A lower trophic level model for the North Pacific marine ecosystem, *Ecol. Modell.*, **202**(1–2), 12–25, doi:10.1016/j.ecolmodel.2006.08.021.
- Kostadinov, T. S., D. A. Siegel, and S. Maritorena (2009), Retrieval of the particle size distribution from satellite ocean color observations, *J. Geophys. Res.*, **114**, C09015, doi:10.1029/2009JC005303.
- Kulk, G., W. H. Van de Poll, R. G. W. Visser, and A. Buma (2011), Distinct differences in photoacclimation potential between prokaryotic and eukaryotic oceanic phytoplankton, *J. Exp. Mar. Biol. Ecol.*, **398**, 63–72, doi:10.1016/j.jembe.2010.12.011.
- Laws, E. A., P. G. Falkowski, W. O. Smith Jr., H. Ducklow, and J. J. McCarthy (2000), Temperature effects on export production in the open ocean, *Global Biogeochem. Cycles*, **14**, 1231–1246, doi:10.1029/1999GB001229.
- Legendre, L., and J. LeFevre (1991), From individual plankton cells to pelagic marine ecosystems and to global biogeochemical cycles, in *Particle Analysis in Oceanography*, edited by S. Demers, pp. 261–300, Springer, Berlin.
- Li, W. K. W., W. G. Harrison, and E. J. H. Head (2006), Coherent assembly of phytoplankton communities in diverse temperate ocean ecosystems, *Proc. R. Soc. B*, **273**, 1953–1960, doi:10.1098/rspb.2006.3529.
- Liu, H., I. Probert, J. Uitz, H. Claustre, S. Aris-Brosou, M. Frada, F. Not, and C. de Vargasa (2009), Extreme diversity in noncalcifying haptophytes explains a major pigment paradox in open oceans, *Proc. Natl. Acad. Sci. U. S. A.*, **106**(31), 12,803–12,808, doi:10.1073/pnas.0905841106.
- Loisel, H., J.-M. Nicolas, A. Sciandra, D. Stramski, and P. A. (2006), Spectral dependency of optical backscattering by marine particles from satellite remote sensing of the global ocean, *J. Geophys. Res.*, **111**, C09024, doi:10.1029/2005JC003367.
- Maloney, C. L., and J. G. Field (1991), The size-based dynamics of plankton food webs. I. A simulation model of carbon and nitrogen flows, *J. Plankton Res.*, **13**(5), 1003–1038, doi:10.1093/plankt/13.5.1003.
- Mann, N. H. (2003), Phages of the marine cyanobacterial picophytoplankton, *FEMS Microbiol. Rev.*, **27**, 17–34, doi:10.1016/S0168-6445(03)00016-0.
- Marañón, E. (2009), Phytoplankton size structure, in *Encyclopedia of Ocean Sciences*, edited by J. H. Steele, K. Turekian, and S. A. Thorpe, Academic, Oxford, U. K.
- Marañón, E., P. M. Holligan, R. Barciela, N. González, B. Mourinho, M. J. Pazó, and M. Varela (2001), Patterns of phytoplankton size structure and productivity in contrasting open-ocean environments, *Mar. Ecol. Prog. Ser.*, **216**, 43–56, doi:10.3354/meps216043.

- Marañón, E., P. Cermeño, M. Latasa, and R. D. Tadonlélé (2012), Temperature, resources, and phytoplankton size structure in the ocean, *Limnol. Oceanogr.*, *57*, 1266–1278, doi:10.4319/lo.2012.57.5.1266.
- Margalef, R. (1967), Some concepts relative to the organisation of plankton, *Oceanogr. Mar. Biol. Annu. Rev.*, *5*, 257–289.
- Margalef, R. (1978), Life-forms of phytoplankton as survival alternatives in an unstable environment, *Oceanol. Acta*, *1*, 493–509.
- Marinov, I., S. C. Doney, and I. D. Lima (2010), Response of ocean phytoplankton community structure to climate change over the 21st century: Partitioning the effects of nutrients, temperature and light, *Biogeosciences*, *7*, 3941–3959, doi:10.5194/bgd-7-4565-2010.
- Markwardt, C. B. (2008), Non-linear least squares fitting in IDL with MPFIT, in *Proceedings of the Astronomical Data Analysis Software and Systems XVIII*, ASP Conf. Ser., 411, edited by D. Bohlender, P. Dowler, and D. Durand, p. 251, Quebec, Canada, Astron. Soc. Pac., San Francisco, Calif.
- McCave, I. N. (1975), Vertical flux of particles in the ocean, *Deep Sea Res. Oceanogr. Abstr.*, *22*, 491–502.
- McLaren, I. A. (1963), Effects of temperature on growth of zooplankton, and the adaptive value of vertical migration, *J. Fish. Res. Board Can.*, *20*(3), 685–727, doi:10.1139/f63-046.
- Michaels, A. F., and M. W. Silver (1988), Primary production, sinking fluxes and the microbial food web, *Deep Sea Res., Part A*, *35*, 473–490, doi:10.1016/0198-0149(88)90126-4.
- Moré, J. (1978), The Levenberg-Marquardt algorithm: Implementation and theory, in *Numerical Analysis*, 105 pp., Springer, Berlin.
- Morel, A., and A. Bricaud (1981), Theoretical results concerning light absorption in a discrete medium, and application to specific absorption of phytoplankton, *Deep Sea Res., Part A*, *28*, 1375–1393, doi:10.1016/0198-0149(81)90039-X.
- Morel, A., Y. Huot, B. Gentili, P. J. Werdell, S. B. Hooker, and B. A. Franz (2007), Examining the consistency of products derived from various ocean color sensors in open ocean (case 1) waters in the perspective of a multi-sensor approach, *Remote Sens. Environ.*, *111*, 69–88, doi:10.1016/j.rse.2007.03.012.
- Mouw, C. B., and J. Yoder (2010), Optical determination of phytoplankton size composition from global SeaWiFS imagery, *J. Geophys. Res.*, *115*, C12018, doi:10.1029/2010JC006337.
- Nair, A., S. Sathyendranath, T. Platt, J. Morales, V. Stuart, M.-H. Forget, E. Devred, and H. Bouman (2008), Remote sensing of phytoplankton functional types, *Remote Sens. Environ.*, *112*(8), 3366–3375, doi:10.1016/j.rse.2008.01.021.
- Parsons, T. R., and C. M. Lalli (2002), Jellyfish populations explosions: Revisiting a hypothesis of possible causes, *La Mer*, *40*, 111–121.
- Peters, R. H. (1983), *The Ecological Implications of Body Size*, Cambridge Univ. Press, Cambridge, U. K.
- Platt, T., and K. L. Denman (1976), The relationship between photosynthesis and light for natural assemblages of coastal marine phytoplankton, *J. Phycol.*, *12*(4), 421–430, doi:10.1111/j.1529-8817.1976.tb02866.x.
- Platt, T., and K. L. Denman (1977), Organisation in the pelagic ecosystem, *Helgoländer Wiss. Meeresunters.*, *30*, 575–581.
- Platt, T., and K. L. Denman (1978), The structure of pelagic marine ecosystems, *Rapp. P. V. Réun. Cons. Int. Explor. Mer*, pp. 60–65.
- Prieur, L., and S. Sathyendranath (1981), An optical classification of coastal and oceanic waters based on the specific spectral absorption curves of phytoplankton pigments, dissolved organic matter and other particulate materials, *Limnol. Oceanogr.*, *26*, 617–689.
- Probyn, T. A. (1985), Nitrogen uptake by size-fractionated phytoplankton populations in the southern Benguela upwelling system, *Mar. Ecol. Prog. Ser.*, *22*, 249–258.
- Quinones, R. A., T. Platt, and J. Rodríguez (2003), Patterns of biomass-size spectra from oligotrophic waters of the Northwest Atlantic, *Prog. Oceanogr.*, *57*, 405–427, doi:10.1016/S0079-6611(03)00108-3.
- Raimbault, P., M. Rodier, and I. Taupier-Letage (1988), Size fraction of phytoplankton in the Ligurian Sea and the Algerian Basin (Mediterranean Sea): Size distribution versus total concentration, *Mar. Microbial Food Webs*, *3*, 1–7.
- Raven, J., and R. Geider (1988), Temperature and algal growth, *New Phytol.*, *110*(4), 441–461.
- Raven, J. A. (1998), Small is beautiful: The picophytoplankton, *Funct. Ecol.*, *12*, 503–513.
- Reynolds, C. S. (1987), Community organization in the freshwater plankton, *Symp. Br. Ecol. Soc.*, *27*, 297–325.
- Riegman, R., B. R. Kuipers, A. A. M. Noordeloos, and H. J. Witte (1993), Size-differential control of phytoplankton and the structure of plankton communities, *Neth. J. Sea Res.*, *31*(3), 225–265.
- Roy, S., T. Platt, and S. Sathyendranath (2011), Modelling the time-evolution of phytoplankton size spectra from satellite remote sensing, *ICES J. Mar. Sci.*, *68*, 719–728, doi:10.1093/icesjms/fsq176.
- San Martín, E., R. P. Harris, and X. Irigoien (2006), Latitudinal variation in plankton size spectra in the Atlantic Ocean, *Deep Sea Res., Part I*, *53*, 1560–1572, doi:10.1016/j.dsr.2.2006.05.006.
- Sathyendranath, S., and T. Platt (2007), Spectral effects in bio-optical control on the ocean system, *Oceanologia*, *49*(1), 5–39.
- Sathyendranath, S., V. Stuart, G. Cota, H. Maas, and T. Platt (2001), Remote sensing of phytoplankton pigments: A comparison of empirical and theoretical approaches, *Int. J. Remote Sens.*, *22*, 249–273, doi:10.1080/014311601449925.
- Sathyendranath, S., L. Watts, E. Devred, T. Platt, C. Caverhill, and H. Maass (2004), Discrimination of diatoms from other phytoplankton using ocean-colour data, *Mar. Ecol. Prog. Ser.*, *272*, 59–68, doi:10.3354/meps272059.
- Schlesinger, D. A., L. A. Molot, and B. J. Shuter (1981), Specific growth rates of freshwater algae in relation to cell size and light intensity, *Can. J. Fish. Aquat. Sci.*, *38*, 1052–1058.
- Serret, P., C. Robinson, E. Fernández, E. Teira, and G. Tilstone (2001), Latitudinal variation of the balance between plankton photosynthesis and respiration in the eastern Atlantic Ocean, *Limnol. Oceanogr.*, *46*(7), 1642–1652, doi:10.4319/lo.2001.46.7.1642.
- Sheldon, R. W., A. Prakash, and W. H. Sutcliffe (1972), The size distribution of particles in the ocean, *Limnol. Oceanogr.*, *17*, 327–340.
- Silió-Calzada, A., A. Bricaud, J. Uitz, and B. Gentili (2008), Estimation of new primary production in the Benguela upwelling area, using ENVISAT satellite data and a model dependent on the phytoplankton community size structure, *J. Geophys. Res.*, *113*, C11023, doi:10.1029/2007JC004588.
- Sunda, W. G., and S. A. Huntsman (1997), Interrelated influence of iron, light and cell size on marine phytoplankton growth, *Nature*, *390*, 389–392, doi:10.1038/37093.
- Thingstad, T. F., and E. Sakshaug (1990), Control of phytoplankton growth in nutrient recycling ecosystems. Theory and Terminology, *Mar. Ecol. Prog. Ser.*, *63*, 261–272.
- Trees, C. C., D. K. Clark, R. R. Bidigare, M. E. Ondrusek, and J. L. Mueller (2000), Accessory pigments versus chlorophyll *a* concentrations within the euphotic zone: A ubiquitous relationship, *Limnol. Oceanogr.*, *45*, 1130–1143, doi:10.4319/lo.2000.45.5.1130.
- Uitz, J., H. Claustre, A. Morel, and S. B. Hooker (2006), Vertical distribution of phytoplankton communities in open ocean: an assessment based on surface chlorophyll, *J. Geophys. Res.*, *111*, C08005, doi:10.1029/2005JC003207.
- Uitz, J., Y. Huot, F. Bruyant, M. Babin, and H. Claustre (2008), Relating phytoplankton photophysiological properties to community structure on large scales, *Limnol. Oceanogr.*, *53*(2), 614–630.
- Uitz, J., H. Claustre, F. Brian Griffiths, J. Ras, N. Garcia, and V. Sandroni (2009), A phytoplankton class-specific primary production model applied to the Kerguelen Islands region (Southern Ocean), *Deep Sea Res., Part I*, *56*, 541–560, doi:10.1016/j.dsr.2008.11.006.

- Uitz, J., H. Claustre, B. Gentili, and D. Stramski (2010), Phytoplankton class-specific primary production in the world's oceans: Seasonal and interannual variability from satellite observations, *Global Biogeochem. Cycles*, *24*, GB3016, doi:10.1029/2009GB003680.
- Veldhuis, M. J. W., K. R. Timmermans, P. Croot, and B. Van Der Wagt (2005), Picophytoplankton; a comparative study of their biochemical composition and photosynthetic properties, *J. Sea Res.*, *53*, 7–24, doi:10.1016/j.seares.2004.01.006.
- Vidussi, F., H. Claustre, B. B. Manca, A. Luchetta, and J. C. Marty (2001), Phytoplankton pigment distribution in relation to upper thermocline circulation in the eastern Mediterranean Sea during winter, *J. Geophys. Res.*, *106*(C9), 19,939–19,956, doi:10.1029/1999JC000308.
- Ward, B. A., S. Dutkiewicz, O. Jahn, and M. J. Follows (2012), A size-structured food-web model for the global ocean, *Limnol. Oceanogr.*, *57*(6), 1877–1891, doi:10.4319/lo.2012.57.6.1877.
- Welschmeyer, N. A. (1994), Fluorometric analysis of chlorophyll *a* in the presence of chlorophyll *b* and pheopigments, *Limnol. Oceanogr.*, *39*(8), 1985–1992.
- Woodworth-Jefcoats, P. A., J. J. Polovina, J. P. Dunne, and J. L. Blanchard (2012), Ecosystem size structure response to 21st century climate projection: Large fish abundance decreases in the central North Pacific and increases in the California Current, *Global Change Biol.*, *19*(3), 724–733, doi:10.1111/gcb.12076.
- Yentsch, C. S., and D. A. Phinney (1989), A bridge between ocean optics and microbial ecology, *Limnol. Oceanogr.*, *34*(8), 1694–1705.
- Zeng, Q., and S. W. Chisholm (2012), Marine viruses exploit their host's two-component regulatory system in response to resource limitation, *Curr. Biol.*, *22*, 124–128, doi:10.1016/j.cub.2011.11.055.